The Journal of Immunology

Regulation of Embryonic Hematopoiesis by a Cytokine-Inducible SH2 Domain Homolog in Zebrafish

Rowena S. Lewis, Suzita M. Noor, Fiona W. Fraser, Robert Sertori, Clifford Liongue and Alister C. Ward

J Immunol 2014; 192:5739-5748; Prepublished online 16 May 2014;
doi: 10.4049/jimmunol.1301376
http://www.jimmunol.org/content/192/12/5739

The Journal of Immunology is published twice each month by
The American Association of Immunologists, Inc.,
9650 Rockville Pike, Bethesda, MD 20814-3994.

Print ISSN: 0022-1767 Online ISSN: 1550-6606.

Regulation of Embryonic Hematopoiesis by a Cytokine-Inducible SH2 Domain Homolog in Zebrafish

Rowena S. Lewis,[*,†,1] Suzita M. Noor,[‡,§,¶,1] Fiona W. Fraser,[‡,§] Robert Sertori,[‡,§] Clifford Liongue,[‡,§] and Alister C. Ward[‡,§]

Cytokine-inducible SH2 domain–containing protein (CISH), a member of the suppressor of cytokine signaling family of negative feedback regulators, is induced by cytokines that activate STAT5 and can inhibit STAT5 signaling in vitro. However, demonstration of a definitive in vivo role for CISH during development has remained elusive. This study employed expression analysis and morpholino-mediated knockdown in zebrafish in concert with bioinformatics and biochemical approaches to investigate CISH function. Two zebrafish *CISH* paralogs were identified, *cish.a* and *cish.b*, with high overall conservation (43–46% identity) with their mammalian counterparts. The *cish.a* gene was maternally derived, with transcripts present throughout embryogenesis, and increasing at 4–5 d after fertilization, whereas *cish.b* expression commenced at 8 h after fertilization. Expression of *cish.a* was regulated by the JAK2/STAT5 pathway via conserved tetrameric STAT5 binding sites ($TTCN_3GAA$) in its promoter. Injection of morpholinos targeting *cish.a*, but not *cish.b* or control morpholinos, resulted in enhanced embryonic erythropoiesis, myelopoiesis, and lymphopoiesis, including a 2- 3-fold increase in erythrocytic markers. This occurred concomitantly with increased activation of STAT5. This study indicates that CISH functions as a conserved in vivo target and regulator of STAT5 in the control of embryonic hematopoiesis. *The Journal of Immunology*, **2014, 192: 5739–5748.**

Cytokines play an integral role in the development and homeostasis of the hematopoietic system (1). For example, erythropoietin (EPO) mediates erythroid development during embryogenesis and maintains appropriate RBC numbers in the adult in response to environmental signals such as hypoxia (2), whereas G-CSF contributes to granulopoiesis, with a key role in "emergency" hematopoiesis (3). To achieve these functions, cytokines bind to specific cell-surface receptors, which then transmit signals to the nucleus by a range of intracellular signaling pathways, particularly the Janus kinase/signal transducer and activator of transcription (JAK/STAT) pathway. An important aspect of the cytokine receptor/JAK/STAT system is the subsequent extinguishing of signaling by a series of negative regulators, such as members of the suppressor of cytokine signaling (SOCS) family of proteins (4). There are eight mammalian SOCS members, SOCS1–7 and the alternatively named cytokine-inducible SH2 domain–containing protein (CISH). Of these, SOCS1–3 and CISH have been shown to act as classical negative feedback regulators, being induced by cytokine receptor/JAK/STAT signaling and then inhibiting signaling via a number of mechanisms (5, 6).

CISH was first identified as an immediate-early gene induced in hematopoietic cells by cytokines that activate STAT5, including EPO, IL-2, and IL-3 (7), but not by a mutant IL-2 receptor that was unable to activate STAT5 (8). Subsequent studies revealed induction of CISH by other cytokines that activate STAT5, such as growth hormone (9), G-CSF (10), and prolactin (11). Indeed, *Stat5a/b*-defective mice showed no detectable *CISH* expression (12, 13), underpinning the key role of STAT5 in *CISH* gene regulation. *CISH* is known to be a direct STAT5 target gene (8), mediated via two sets of tandem STAT5 binding sites present in the *CISH* promoter (14).

Similar to other members of the SOCS family, the CISH protein contains a divergent N-terminal region, a centrally located SH2 domain, and a conserved C-terminal SOCS box domain (4, 7). CISH binds via its SH2 domain to phosphorylated tyrosine residues of activated cytokine receptors, where it suppresses signaling via at least two mechanisms. First, CISH is able bind to the same receptor phosphotyrosine residues as STAT5 and thereby physically block STAT5 docking, as has been shown for both the EPO receptor (EPOR) (15) and the growth hormone receptor (16). Second, CISH can facilitate proteasomal degradation of activated receptor complexes via interactions with Cullin 5 and Elongin B/C (17). Enforced CISH expression in vitro inhibited EPO-dependent activation of STAT5 and partially suppressed EPO-mediated cell proliferation, indicating a specific negative role in STAT5 signal transduction (7, 8). CISH was also found to promote apoptosis of erythroid progenitor cells ex vivo, consistent with an antagonistic role of STAT5, a known antiapoptotic factor (18).

*School of Life and Environmental Sciences, Deakin University, Burwood, Victoria 3125, Australia; †Walter and Eliza Hall Institute for Medical Research, Parkville, Victoria 3050, Australia; ‡School of Medicine, Deakin University, Geelong, Victoria 3217, Australia; §Strategic Research Centre in Molecular and Medical Research, Deakin University, Geelong, Victoria 3217, Australia; and ¶Faculty of Medicine, University of Malaya, 50603 Kuala Lumpur, Malaysia

[1]R.S.L. and S.M.N. contributed equally to this work.

Received for publication May 23, 2013. Accepted for publication April 9, 2014.

This work was supported by Deakin University postgraduate research awards (to R.S.L. and R.S.) and the Alfred Deakin Fellowship (to C.L.) and funding from the Malaysian Ministry of Higher Education and the University of Malaya (to S.M.N.). This work was also supported by an Australian Research Council discovery project (to A.C.W.) and it utilized the resources of FishWorks, a collaborative infrastructure for zebrafish research, which is an Australian Research Council linkage infrastructure, equipment, and facilities initiative (to A.C.W.).

The sequences presented in this article have been submitted to GenBank (http://www.ncbi.nlm.nih.gov) under accession numbers FR749998, FR749999, HE863767, and HE 863768.

Address correspondence and reprint requests to Prof. Alister C. Ward, School of Medicine, Deakin University, Pigdons Road, Geelong, VIC 3217, Australia. E-mail address: award@deakin.edu.au

The online version of this article contains supplemental material.

Abbreviations used in this article: CISH, cytokine-inducible SH2 domain–containing protein; dpf, days postfertilization, EPO, erythropoietin; EPOR, EPO receptor; HEK, human embryonic kidney; hpf, h postfertilization; LNA, locked nucleic acid; qRT^2-PCR, quantitative real-time RT-PCR; SOCS, suppressor of cytokine signaling; WISH, whole-mount in situ hybridization.

Transgenic mice engineered to express *CISH* under the control of the β-actin promoter exhibited growth retardation, defective mammary gland development, and altered T and NK cell responses (19). These phenotypes were consistent with those observed in *Stat5a/b*-defective mice (12, 13), and they suggested a specific role in the regulation of STAT5 in vivo. Indeed, transgenic CISH expression suppressed STAT5 activation induced by both IL-2 (20) and prolactin (21). An alternate transgenic mouse model in which *CISH* was expressed in a T cell–specific manner indicated an independent role in TCR signaling (20). Meanwhile, increased susceptibility to infectious diseases has recently been associated with polymorphisms in the human *CISH* promoter, which blunted *CISH* induction following IL-2 stimulation (22).

A *Cish* knockout mouse has recently been described, but its analysis was restricted to adult lymphopoiesis, in which it participates in Th cell differentiation mediated by IL-4 (23). Therefore, much remains to be determined about the normal developmental function of CISH. The zebrafish has proven to be an informative model for the study of hematopoiesis, with considerable conservation with mammals, including the presence of distinct waves of development (24). The earliest zebrafish hematopoietic cells are derived from hemangioblasts in the lateral plate mesoderm (25), characterized by the expression of markers for hematopoietic progenitors, such as *scl* and *ikaros*, as well as those for early myeloid (*spi1*) and erythroid (*gata1*) populations (26–29). From these progenitors, distinct populations are generated that become foci for myeloid and erythromyeloid progenitor production. Rostrally, macrophage cells are generated expressing lysozyme (*lyz*) (30) while caudally erythroid cells expressing β-embryonic globin (*β-e-globin*) (31) and heterophilic granulocytes expressing *mpo* and *mmp9* (32, 33) are produced. Definitive hematopoietic stem cells expressing *c-myb* emerge in the dorsal aorta (34), and following a transient phase within the caudal hematopoietic tissue (35), they populate the developing kidney, the major adult hematopoietic site, and the thymus, where early lymphoid precursors expressing *ikaros* (27) give rise to mature T cells, expressing markers such as *rag1* and *tcra* (36). Zebrafish has also been shown to possess homologs for JAK2 and STAT5, as well as the relevant upstream cytokine receptors (37–40). Therefore, to gain insight into the role played by CISH in vivo we have employed bioinformatics and biochemical approaches together with expression analysis and morpholino-mediated knockdown in zebrafish.

Materials and Methods

Identification and analysis of CISH homologs from zebrafish

Zebrafish ESTs encoding proteins with homology to human CISH were identified using BLASTX (41), sequenced in full, and assembled along with relevant expressed sequence tag sequences into contigs using Sequencher (Gene Codes, Ann Arbor, MI). Two distinct genes were found that both encoded proteins with high homology to CISH and were named *cish.a* and *cish.b* according to guidelines of the Zebrafish Nomenclature Committee, with their respective full-length nucleotide sequences deposited in GenBank (http://www.ncbi.nlm.nih.gov; *cish.a*, accession no. FR749998; *cish.b*, accession no. FR749999). Protein sequence alignment of cish.a and cish.b with *Homo sapiens* CISH (NP_037456.5) was performed using pairwise BLAST. Multiple sequence alignments were performed using the ClustalX program (42) with human CISH (AAH31590), SOCS1 (NP_003736), SOCS2 (NP_003868), and SOCS3 (CAG46495); *Mus musculus* (mouse) Cish (BAA06713), Socs1 (NP_034026), Socs2 (AAI06154), and Socs3 (NP_031733); *Gallus gallus* (chicken) cish (NP_989957), socs1 (NP_001131120), socs2 (NP_989871), and socs3 (NP_989931); *Xenopus tropicalis* (western clawed frog) cish (AAI71013), socs1 (AAH88083), socs2 (NP_01120898), and socs3 (AAH75262); *Tetraodon nigroviridis* (pufferfish) cish.a (ABM68026) and cish.b (ABM68031); and *Ciona intestinalis* (sea squirt) socs.a (BAE06701.1). A phylogenic tree was derived from this alignment using the neighbor-joining algorithm (43) and visualized in TreeView (44). Genomic sequences corresponding to the zebrafish *cish.a* and *cish.b* genes were identified by BLASTN searching of zebrafish genomic sequences at GenBank and the positions of intron/exon boundaries determined by alignment with the corresponding zebrafish *cish* cDNA sequence, applying the "GT-AG" rule (45). The genomic arrangement of the human and zebrafish *CISH* loci, along with syntenic genes, was determined using National Center for Biotechnology Information Map Viewer. The zebrafish *cish.a* and *cish.b* promoters were deposited at GenBank (http://www.ncbi.nlm.nih.gov) under accession nos. HE863767 (*cish.a*) and HE863768 (*cish.b*).

Zebrafish husbandry and manipulation

Wild-type zebrafish were maintained using standard husbandry practices. Embryos at the first through fourth cell stages were injected with 1 mM antisense morpholinos diluted in 1× Danieau buffer (58 mM NaCl, 0.7 mM KCl, 0.4 mM $MgSO_4$, 0.6 mM $CaCl_2$, 5.0 mM HEPES [pH 9]) or in vitro–transcribed mRNA encoding constitutively active stat5.1 (46) or cish.a diluted to 100 ng/μl. Morpholinos used were cish.a^{SS} (5′-AATTCTGTTTTCATCTACCTGAGGC-3′), cish.a^{ATG} (5′-GCCTTCAACGCACAATATCATAAT-3′), cish.b^{ATG} (5′-ACTGGTTCCTCTTTGTGGGCATTAA-3′), stat5.1^{SS} (5′-GTGAACTTGTGACTTACCAGAGTTG-3′), and standard control morpholino (5′-CCTCTTACCTCAGTTACAATTTATA-3′). Embryos were also treated with the JAK2 inhibitor AG490 (30 μM), as described previously (47). Institutional and national guidelines for the care and use of laboratory animals were followed in all studies.

In vitro transcription and translation

RNA was transcribed in vitro from linearized plasmid templates using the T7 mMessage mMachine kit (Ambion, Austin, TX) for embryo injection. Alternatively, coupled in vitro transcription/translation was carried out with the TNT-T7 quick coupled transcription/translation systems (Promega, Madison, WI) using 1 μg linearized *cish.a* plasmid and 100 ng cish.a^{ATG} or scrambled morpholino and incubated for 90 min at 30°C.

Western blot analysis

In vitro translation products were analyzed via SDS-PAGE and transferred to polyvinylidene difluoride and detected using the Transcend nonradioactive translation detection system (Promega). Western blot analysis of zebrafish embryos with anti–phospho-STAT5 Abs was performed as described previously (47).

RNA isolation

Total RNA was extracted from zebrafish embryos or adult tissues using TRIzol reagent (Life Technologies, Rockville, MD) following the manufacturer's recommendations and resuspended in nuclease-free water.

RT-PCR

Total RNA was subjected to either standard RT-PCR or quantitative real-time RT-PCR (qRT^2-PCR) (47). Primers used were (forward and reverse, respectively): *lmo2*, 5′-GGAAAACACTGGAGGCAAATGAGG-3′ and 5′-GGTCCACACAAAAATGTCCTGCTC-3′; *scl*, 5′-GGCCAGTTCATAGAGGGTCA-3′ and 5′-TCCCATAGGATTGCATTGGT-3′; *runx1*, 5′-AGAAGCCGGATGAAGCAGTA-3′ and 5′-ATACGACCAGGATGGAGACG-3′; *gata1*, 5′-CTCCTCTGAGCCTTCTCGTTGG-3′ and 5′-GTCTGATGAGGGGTCTGTTCTGGC-3′; *spi1*, 5′-GACCAAGAGCAGGGCAG-3′ and 5′-CATTACCTTCAACACTGAGTTCAA-3′; *epor*, 5′-GCCCTGTTCTTCACCTCTCTGG-3′ and 5′-CTTCTGCTCTGGTGTTGGTATGTC-3′; *β-e-globin*, 5′-ATCTTCGCCAAGGCTGACTA-3′ and 5′-GCATAGGTGGCCTTGATGTT-3′; *epo*, 5′-TACTGCTGATGGTGCTGGAG-3′ and 5′-GACTGGACCTCCTGAGCTTG-3′; *cish.a*, 5′-TCACCGAGACGCATTGACGAACC-3′ and 5′-AGACTGAAACGACATTGCCTG-3′; *cish.b*, 5′-CAGTCAGGAATGGTTACAAGGG-3′ and 5′-TATGCGGATGTTAGTAGGGC-3′; *socs1*, 5′-TGGAAGCGGCGACGAGAGTT-3′ and 5′-CGGCTTGAAATGTGTCTGG-3′; *socs2*, 5′-GTGCTGGTCAAACCCAAACT-3′ and 5′-TTGGGCAAAGGAAGTTCTTG-3′; *socs3a*, 5′-GAGACTCATAGGCTCTTTTGACCAG-3′ and 5′-CTCTTTCCCGCTGATGGC-3′; *socs3b*, 5′-TGAGTCGGATAACGCTTTGA-3′ and 5′-GTCAAGCCTACTATGCGTTACC-3′; *tcra*, 5′-ACTGAAGTGAAGCCGAAT-3′ and 5′- CGTTAGCTCATCCACGCT-3′; *lck*, 5′-CAAGCCTCCAGTCAGTCAGA-3′ and 5′- GCGTCATTCCTGGAGAGA-3′; *foxn1*, 5′-GGCACTGATGTGGAGACC-3′ and 5′- TTAGGGTACAGTGGTTGAGGA-3′; and *β-actin*, 5′-TGGCATCACACCTTCTAC-3′ and 5′-AGACCATCACCAGAGTCC-3′. Each primer set flanked splice sites such that amplification of contaminating genomic DNA would produce much larger fragments in each case.

Whole-mount in situ hybridization and histological analysis

Embryos were dechorionated and fixed for 2–4 d in 4% (w/v) paraformaldehyde at 4°C prior to whole-mount in situ hybridization (WISH) with

DIG-labeled antisense probes (48), or alternatively using a double DIG-labeled locked nucleic acid (LNA) oligonucleotide probe to *cish.a*, 5′-DigN-TGATGACCAAGCGAGTGAGAT-DigN-3′ (Exiqon).

Quantitation was achieved by counting of positive cells or using the thresholding tool in ImageJ (49) as appropriate, on at least 30 embryos. *O*-dianisidine staining was performed on freshly anesthetized embryos as described (32). Blood smears were prepared from 48 h postfertilization (hpf) embryos and stained with May–Grünwald–Giemsa (Sigma-Aldrich, Sydney, NSW, Australia), with quantitation of specific cell populations performed by hand on randomly selected samples using a dissecting microscope as described previously (46), and analyzed using a Student *t* test.

Northern blot analysis

Total RNA (15 μg) was loaded onto an agarose/formaldehyde gel and run at 80 V for 1 h before being transferred to Hybond-N+ (Amersham Biosciences, Uppsala, Sweden) overnight in 10× SSC. Membranes were rinsed briefly in 2× SSC and prehybridized in QuikHyb (Stratagene, La Jolla, CA) for 30 min at 62°C, followed by the addition of ∼200 cpm [^{32}P]-labeled full-length *cish.a* probe and incubation for 1 h. Membranes were subsequently washed in 2× SSC and exposed to a Fujifilm imaging plate (BAS-IP MS 2325) and viewed on a Fujifilm BAS1800II (Berthold Industries, Melbourne, VIC, Australia) after a 2-wk exposure.

Transfection

Human embryonic kidney (HEK) 293T cells were cultured in DMEM/10% (v/v) FCS at 37°C and 10% (v/v) CO_2. These were transiently transfected with constitutively active zebrafish stat5.1 (H298R/N714F) (46) and hyperactive jak2a (E629K) (47) at 80% confluence using a 3:1 ratio of DNA/FuGENE 6 reagent (Roche Diagnostics, Indianapolis, IN) and incubated for 2 d before harvesting.

EMSA

Nuclear extracts were prepared from ∼10^6 transfected cells washed with 1 ml ice-cold PBS containing 0.1 mM Na_3VO_4 or 30 pooled zebrafish embryos physically disrupted with a Teflon pestle in a 1.5-ml plastic tube. Extracts were incubated with 1 μg poly(deoxyinosinic-deoxycytidylic) acid (Sigma-Aldrich) and ∼200 cpm [^{32}P]-labeled double-stranded probes in 1× Lamb binding buffer (10 mM HEPES [pH 7.6], 17 mM NaCl, 3 mM $NaMoO_4$, 0.85 mM DTT, 5% glycerol, 0.15 mM $MgCl_2$) at room temperature for 20–30 min. Probes were zebrafish *cish.a* distal STAT5 binding sites (5′-CACTTTTCCTGGAAAGTTCTTGGAACGT-CA-3′), zebrafish *cish.a* proximal STAT5 binding sites (5′-GATTCTCA-GAAAAGCAATCCCGAGAAGT-3′), and the high-affinity mouse *β-casein* STAT5 binding site (5′-AGATTTCTAGGAATTCAATCC-3′). Samples were loaded onto a 4% acrylamide/1/2× TBE vertical gel, which was run at 100 V for 2 h before drying and exposing overnight to a Fujifilm imaging plate (BAS-IP MS 2325) for subsequent viewing on a Fujifilm BAS1800II (Berthold Industries).

Results

Identification and characterization of zebrafish CISH homologs

Extensive searching of zebrafish gene databases with human *CISH* identified two homologous genes, which were designated *cish.a* and *cish.b*. Phylogenetic analysis of their encoded proteins confirmed that both formed a distinct clade with other vertebrate CISH proteins, but not the closely related SOCS1, SOCS2, or SOCS3 (Fig. 1A). Additionally, *cish.a* and *cish.b* showed conserved synteny (Fig. 1B) and splicing (Fig. 1C) with human *CISH*, and both zebrafish genes possessed multiple destabilization motifs ($AT_{3-4}A$) in their 3′ untranslated region, as found in their human counterpart (7). The encoded proteins showed the typical three domain structure found in all SOCS family proteins (Supplemental Fig. 1). Compared to human CISH, the cish.b protein (43% identity) was slightly more divergent than cish.a (46% identity), especially in the N-terminal domain (Fig. 1D). These domains were shorter in each case than for human CISH, but each retained a high frequency of PEST residues (>30%), which are associated with rapid protein turnover. The SH2 and SOCS box domains showed very high identity, indicative of functional conservation. Collectively, these data suggested that *cish.a* and *cish.b* represented authentic paralogs of the mammalian *CISH* genes.

Analysis by qRT^2-PCR revealed that both *cish.a* and *cish.b* were expressed during embryogenesis (Fig. 1E). Transcripts for *cish.a* were strongly evident at the single-cell stage, indicative of maternal derivation, but decreased significantly by 8 hpf. Transcripts were present at a lower level throughout embryogenesis, with a significant increase from 4 to 5 d postfertilization (dpf) that continued to 7 dpf. In contrast, *cish.b* was not maternally derived, but transcripts were detected from 8 hpf and persisted throughout embryogenesis, with an increase from ∼3–4 dpf. WISH of zebrafish embryos detected maternal *cish.a* transcripts (Fig. 1F) but produced little staining at other time points for either *cish* gene, presumably due to low levels of expression. However, using an LNA probe, expression of *cish.a* was observed in the aorta-gonad-mesonephros region at 32 hpf, the pronephric ducts at 3 dpf, and with an RNA probe in the thymus at 5 dpf (Fig. 1F).

Targeted knockdown of zebrafish cish *genes*

To analyze the possible role of the two *cish* paralogs during embryogenesis, antisense morpholinos were designed to target the start codons of *cish.a* and *cish.b* to inhibit protein translation, designated cish.a^{ATG} and cish.b^{ATG}, respectively (Fig. 2A, 2E). To verify the specificity of the phenotypes observed with cish.a^{ATG}, a second antisense morpholino was designed that targeted the splice donor site of exon 2/intron 2 of *cish.a* to inhibit splicing, named cish.a^{SS}. The effectiveness of cish.a^{ATG} was confirmed in an in vitro transcription/translation assay, with the cish.a^{ATG} morpholino robustly blocking translation in contrast to a scrambled control morpholino (Fig. 2B). For cish.a^{SS}, RT-PCR with primers spanning the splice site yielded a single product of the expected size in control embryos that was not present in those injected with the cish.a^{SS} morpholino, which instead produced a slightly larger product (Fig. 2C). Sequencing revealed that this was due to utilization of an alternative downstream splice donor site in the morphants, resulting in the inclusion of 25 bp intronic sequence that contained an in-frame stop codon, which would encode a truncated protein product consisting of just 51 aa of the N-terminal domain but lacking the functional SH2 and SOCS box domains (Fig. 2D).

Analysis of zebrafish embryos injected with these morpholinos showed no major developmental defects. However, at 24 hpf embryos injected with either *cish.a* morpholino showed expansion of the rostral blood island, a site of early hematopoiesis in zebrafish embryos (Fig. 2F, 2G), which had largely dissipated by 48 hpf (Fig. 2I, 2J), with no obvious difference at 4 dpf (Fig. 2L, 2M). Instead, increased RBCs were observed by light microscopy at 48 hpf in *cish.a* morphants, which was confirmed by *O*-dianisidine staining of hemoglobin (Fig. 2N, 2O). This increase was no longer evident by 6 dpf (Fig. 2Q, 2R). These phenotypes were not observed in *cish.b* morphants (Fig. 2H, 2K, 2P).

Characterization of hematopoiesis in cish.a *morphants*

To further investigate the hematopoietic perturbations in *cish.a* morphants, qRT^2-PCR was performed at 12 hpf for the early hematopoietic progenitor markers *lmo2* (50), *scl* (51), and *runx1* (52), the early erythroid marker *gata1* (53), and the early myeloid marker *spi1* (54). No significant differences were observed (Fig. 3A), a result that was confirmed by WISH (Fig. 3B–G and data not shown). By 18 hpf, expression of *scl* and *gata1* remained unaltered by WISH (Fig. 3H–K), but there was increased expression of the erythoid marker *epor* (55) (Fig. 3L, 3M). By 24 hpf, there was significant upregulation of *ikaros*, which serves as a marker of hematopoietic progenitors at this time point (27) (Fig. 3N–P, 3T), as well as *gata1* (Fig. 3V) and the mature erythroid marker *β-e-globin* (31) (data not shown), whereas *epor* (Fig. 3Q–S, 3U) remained elevated. However, real-time expression

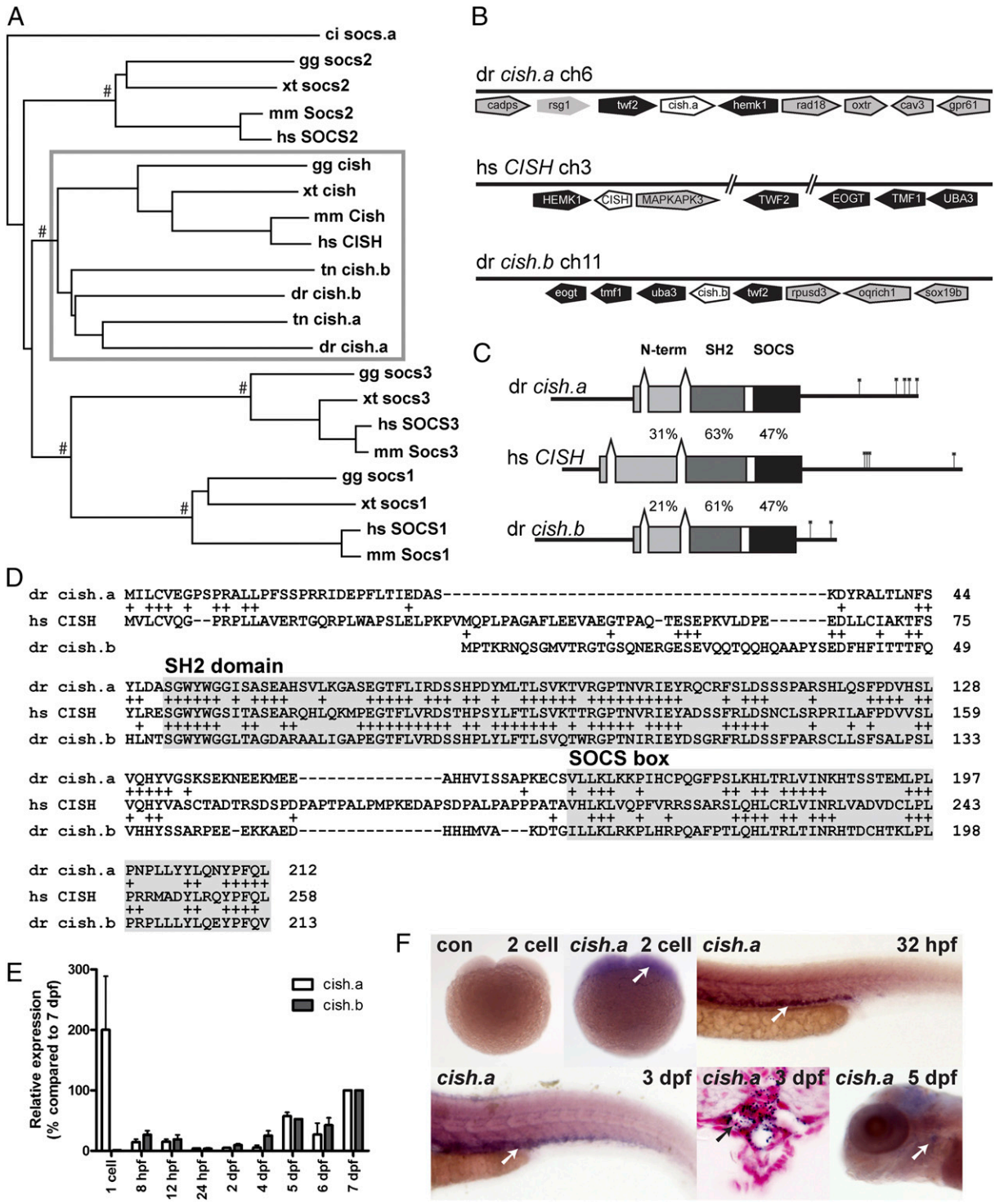

FIGURE 1. Characterization of zebrafish *cish* genes. (**A**) Phylogenic analysis of CISH proteins. A phylogenetic tree was constructed from a ClustalX alignment of zebrafish (*Danio rerio*, dr) and pufferfish (*Tetraodon nigroviridas*, tn) cish.a and cish.b proteins with the CISH, SOCS1, SOCS2, and SOCS3 proteins from human (*Homo sapiens*, hs), (*Mus musculus*, mm), Western clawed frog (*Xenopus tropicalis*, xt), and chicken (*Gallus gallus*, gg), along with socs.a from sea squirt (*Ciona intestinalis*, ci) as an outgroup, using the Neighbor Joining program and visualized with the TreeView program. Key branches having bootstrap values >800 are indicated with hash symbols, with the CISH clade highlighted with a gray box. (**B**) Conserved synteny of *cish* genes. Synteny analysis of zebrafish (dr) *cish.a* and *cish.b* and human (hs) *CISH* gene loci with adjacent genes indicated. (**C**) Conserved structure and splicing of *cish* genes. Schematic comparison of the zebrafish (dr) *cish.a* and *cish.b* genes with human (hs) *CISH*, showing splicing structure and conserved domains with the extent of identity of each indicated as a percentage. The relative position of the $AT_{3-4}A$ destablization motifs in the 3′ untranslated region of each gene are indicated. (**D**) Alignment of zebrafish cish sequences with human CISH. Proteins encoded by the *cish.a* and *cish.b* paralogs from zebrafish (dr) and the *CISH* gene from human (hs) were aligned using BLAST. Identical residues are indicated with a cross; the SH2 domain and SOCS box are shaded. (**E**) Expression of *cish* genes during embryogenesis. Total RNA was prepared from embryos at the indicated times after fertilization and used as a template for qRT^2-PCR with primers specific for *cish.a* and *cish.b*. Results were normalized relative to *β-actin* and are shown relative to expression at 7 dpf. (**F**) Spatiotemporal analysis of *cish.a* expression. Embryos at the ages indicated were subjected to WISH with control sense (con) or anti-sense *cish.a* probe, either RNA (two cells, 5 dpf) or LNA (32 hpf, 3 dpf). Arrows point to areas of *cish.a* expression, including in section through 3 dpf embryo (original magnification ×40, black arrow).

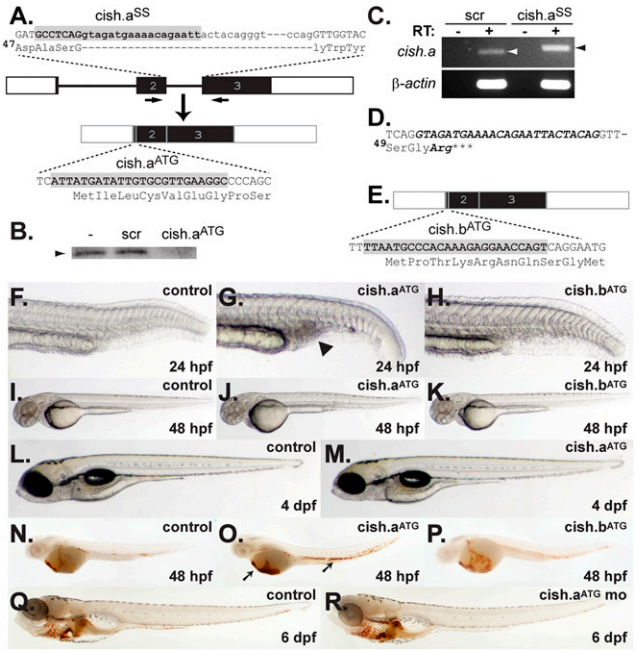

FIGURE 2. Targeted knockdown of zebrafish *cish* genes. (**A**) Schematic representation of the *cish.a* gene and its targeting with morpholinos. Exons are numbered and indicated as boxes, with the coding regions shaded black and introns indicated with a line. Relevant nucleotide, and encoded amino acid, sequences are shown, with exonic sequences in uppercase and intronic sequences in lowercase. Sequences targeted by the respective morpholinos (cish.a^{SS} and cish.a^{ATG}) are bolded and shaded, and the positions of primers used for RT-PCR are indicated with arrows. (**B**–**D**) Analysis of *cish.a* morpholino targeting. For cish.a^{ATG}, *cish.a* mRNA was transcribed and translated in the presence of scrambled (scr) or cish.a^{ATG} morpholino, and the products were detected by Western blot (B). For cish.a^{SS}, total RNA was prepared from embryos injected with scrambled (scr) or cish.a^{SS} morpholino at 24 hpf, incubated in the presence (+) or absence (−) of reverse transcriptase (RT) and subjected to PCR with primers specific for *cish.a* and *β-actin*, as shown (C). The white arrow indicates the wild-type transcript; the black arrow indicates a novel transcript in the cish.a^{SS} morpholino-injected embryos encoding a truncated protein, the relevant sequence of which is shown (D). (**E**) Schematic representation of the *cish.b* gene and its targeting with morpholino, depicted as described in (A). (**F**–**M**) Phenotypic analysis of morphant embryos. Embryos injected with standard control (control) (F, I, and L), cish.a^{ATG} (G, J, and M), or cish.b^{ATG} (H and K) morpholino as viewed under light microscopy at the times indicated. The black arrowhead indicates the expanded posterior blood island. Embryos are of lateral view, with anterior to the left. (**N**–**R**) Hemoglobin staining of morphant embryos with *O*-dianisidine. Embryos injected standard control (control) (N and P), cish.a^{ATG} (O and R), or cish.b^{ATG} (P) morpholinos were stained with *O*-dianisidine at the times indicated and visualized with light microscopy. Black arrows indicate increased RBCs. Embryos are of lateral view, with anterior to the left.

analysis revealed that the increased expression of the erythroid markers *epor* and *β-e-globin* was transient, peaking ~2-fold and 3-fold higher, respectively, at 24 hpf and then returning to basal levels by 72 hpf (Fig. 3W), consistent with the *O*-dianisidine staining. In contrast, there was no significant change in the expression of *epo* (55), indicating it was not responsible. Blood smears from *cish.a* morphants further revealed more proerythroblasts at 48 hpf that was partially sustained at 5 dpf (Fig. 3X, 3Y), although there was no change in cell morphology (Fig. 3Z).

The *cish.a* morphants showed increased staining with the granulocytic marker *mmp9* at 18 hpf (Fig. 4A). Elevated numbers of myeloid cells expressing *spi1* were also observed at 24 hpf (Fig. 4C, 4D), as well as those positive for the mature myeloid cell markers *gcsfr* (56) (Fig. 4E, 4F, 4I) and *lyz* (30) (Fig. 4G, 4H, 4J), with expression of *runx1* also increased at 24 and 48 hpf (Fig. 4K). By 48 hpf, the number of cells positive for *lyz* (Fig. 4L, 4M, 4R) and *mmp9* (Fig. 4N, 4O, 4S), which represent pan-leukocytic markers at this time point, or the granulocytic marker *mpo* (32) (Fig. 4P, 4Q, 4T), were no longer statistically elevated. However, expression of *lyz* and *mmp9* were significantly increased at 4 dpf (Fig. 4U). As a corollary, there was a significant increase in monocytes in the blood at 48 hpf that was lessened by 5 dpf (Fig. 3X, 3Y).

There was no change in the number of *ikaros*-positive lymphoid progenitors in the thymus (27) at 3.5 dpf in *cish.a* morphants (Fig. 4V, 4W). In contrast, by 4 dpf these showed increased expression of *ikaros* (Fig. 4B′), as well as the late lymphoid markers *tcra*, *foxn1, lck*, and *rag1* (36, 57, 58) (Fig. 4X–Z, 4A′, 4B′), indicating an increase in mature T cells. Expression of *ikaros* and *rag1* in the thymus remained raised at 5 dpf (Fig. 4C′–F′), with numbers of lymphoid cells in circulation also increased at this time point, although failing to reach significance (Fig. 3X, 3Y).

Finally, embryos were coinjected with the cish.a morpholinos along with a morpholino-resistant *cish.a* mRNA. This largely rescued the altered expression of *ikaros*, *β-e-globin*, and *mmp9* (Fig. 4G′) seen in *cish.a* morphants, thereby confirming the specificity of the phenotypic changes.

Interactions between zebrafish cish.a *and the JAK2/STAT5 pathway*

A number of studies have identified the JAK2/STAT5 pathway as a key regulator of mammalian *CISH* genes, mediated by JAK2-induced STAT5 binding to four consensus binding sites ($TTCN_3GAA$) in the *CISH* promoter: a proximal pair and a distal pair (8), with the latter arranged to facilitate tetrameric STAT5 binding (14). Analysis of the zebrafish *cish.a* promoter revealed the complete conservation of the distal binding sites and significant conservation of the proximal binding sites (Fig. 5A). In contrast, the *cish.b* promoter totally lacked the distal sites, although the proximal sites were present. To test the functionality of the two tandem sites identified in the *cish.a* promoter, HEK293 cells were transfected with hyperactive zebrafish jak2a (47) with and without wild-type stat5.1 (38), and nuclear extracts were analyzed by EMSAs for their ability to bind to these sites. This revealed that jak2a-activated zebrafish stat5.1 was able to bind to both the proximal and distal binding sites in vitro (Fig. 5B).

To directly confirm that the *cish.a* gene was responsive to stat5.1 in vivo, *cish.a* expression was analyzed in embryos in which stat5.1 was knocked down by morpholino, or in which the upstream JAK2 kinase was inhibited using a pharmacologic inhibitor, AG490 (Fig. 5C). In each case, a significant decrease in *cish.a* expression was observed, whereas *cish.b* levels were not significantly altered. As a corollary, zebrafish embryos were injected with capped RNA encoding constitutively active (H298R/N714F) zebrafish stat5.1 (46). Northern blot analysis of total RNA extracted at 24 hpf failed to detect *cish.a* transcripts in uninjected embryos, consistent with the WISH studies, but *cish.a* transcripts were clearly evident in embryos expressing constitutively active stat5.1 (Fig. 5D). Collectively, this indicates a conserved role for the JAK2/STAT5 pathway in regulating *cish.a*.

Several of the *cish.a* morphant phenotypes were reminiscent of those observed in embryos injected with constitutively active *stat5.1* (46). To investigate this further, protein extracts were prepared from *cish.a* morphants and subjected to Western blot analysis with anti–phospho-STAT5, as described previously (47). This revealed increased STAT5 activation in *cish.a* morphants (Fig. 5E). Several members of the SOCS family, including *CISH*, *SOCS1*, and *SOCS2*, are known to be regulated by STAT5 (5). qRT^2-PCR expression analysis showed that *cish.a*, *socs1*, and *socs2*, but not *cish.b*, *socs3a*, or *socs3b*, were significantly increased by 2- to 3-fold in *cish.a* morphants (Fig. 5F). This supports the hypothesis that cish.a

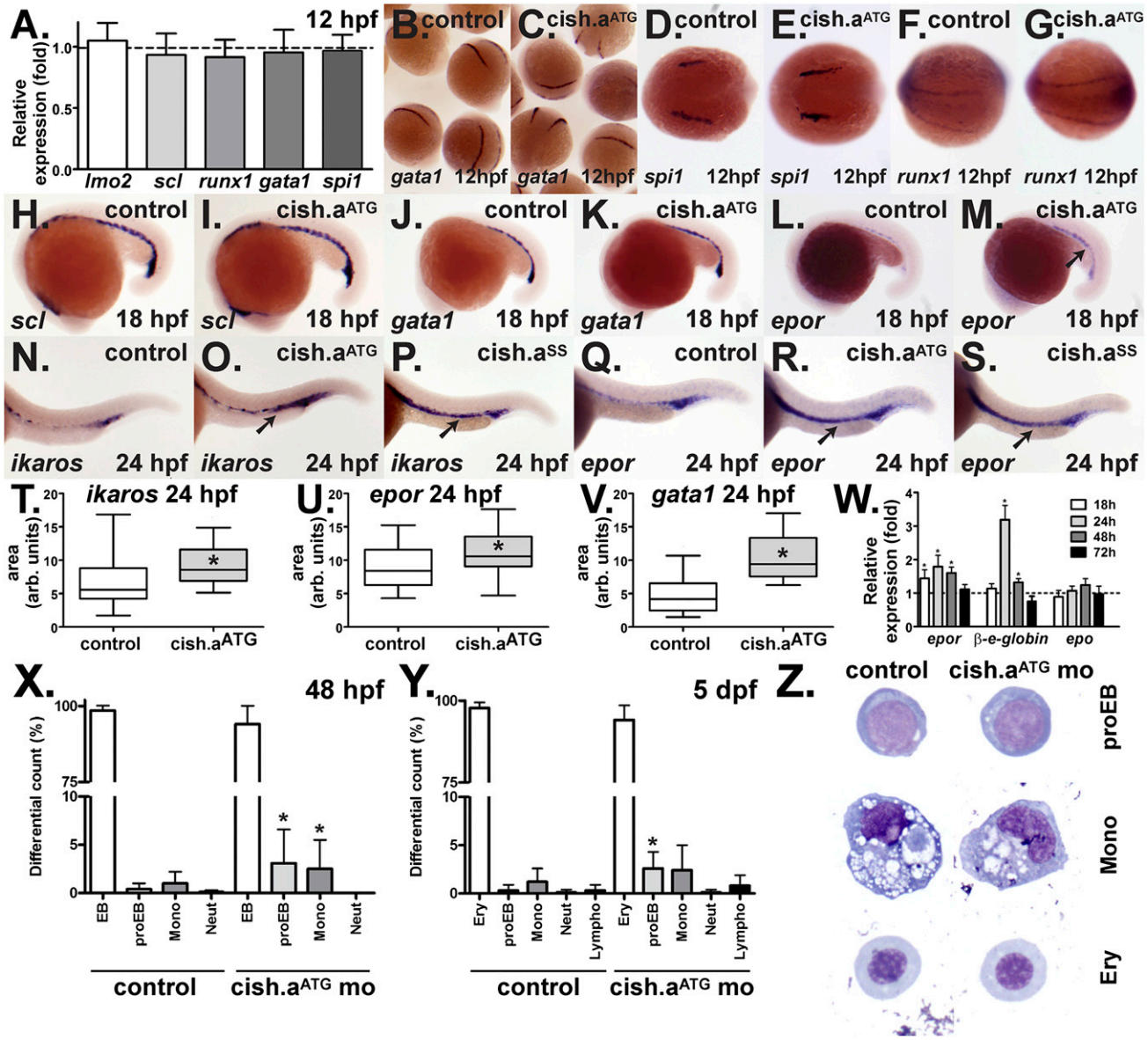

FIGURE 3. Effect of *cish.a* knockdown on early hematopoietic and erythroid markers. (**A** and **W**) qRT^2-PCR analysis of morphant embryos. Total RNA was extracted from embryos injected with standard control or cish.a^{ATG} morpholino and subjected to qRT^2-PCR for the indicated early hematopoietic genes at 12 hpf (A) or the indicated erythroid genes at 18, 24, 48, and 72 hpf (W). In each case, expression was normalized relative to *β-actin*, with mean and SEM shown, and statistical significance indicated (*$p < 0.05$). (**B**–**S**) WISH analysis of morphant embryos. Embryos injected with either standard control or indicated cish.a morpholino were subjected to WISH at the time points and with the probes indicated. Embryos are of lateral view with anterior to the left, except for panels (B)–(G). Arrows indicate increased staining in cish.a morphants, with embryos shown being representative of $n > 150$ in each case, derived from at least three independent experiments. (**T**–**V**) Quantitation of WISH staining. The area of staining (T–V) was determined for at least 30 embryos from a representative experiment for standard control and *cish.a* morphant groups for the marker/time point combinations indicated. Data are presented as a box-and-whiskers graph, showing mean and range, with statistically significant differences indicated (*$p < 0.05$). (**X**–**Z**) Analysis of blood from *cish.a* morphant embryos. Blood samples were prepared from embryos injected with standard control (control) or cish.a^{ATG} morpholino and stained with Wright–Giemsa (original magnification ×100). Differential quantitation of blood cell types was performed at 48 hpf (X) and 5 dpf (Y), with representative proerythroblasts (proEB), monocyte/macrophages (Mono), and erythrocytes (Ery) shown (Z).

negatively regulates STAT5 activity in vivo, with the effects of *cish.a* knockdown due, at least in part, to this increased activity.

Discussion

The SOCS proteins represent key negative regulators of cytokine and growth factor signaling, with the ablation of specific SOCS genes resulting in severe developmental and physiologic disruption (5, 6). Despite CISH being the first member of the SOCS family identified and extensive functional analysis undertaken in vitro, no developmental phenotypes have been ascribed to *Cish* knockout mice, meaning that the in vivo role of CISH has remained unclear. In this study, use of the zebrafish developmental model has provided definitive evidence for the participation of CISH in the regulation of embryonic hematopoiesis.

Two paralogs of *CISH* were found in zebrafish, *cish.a* and *cish.b*, whose encoded proteins showed the typical three-domain structure of other SOCS proteins (4), and also retained signals responsible for rapid turnover of both the transcript and the encoded protein. A previous study reported almost equivalent zebrafish sequences to *cish.a* and *cish.b*, but designated them *cish* and *socs8*, respectively (59). However, owing to the high degree of sequence homology to their mammalian counterparts, and conserved syntenic relationships,

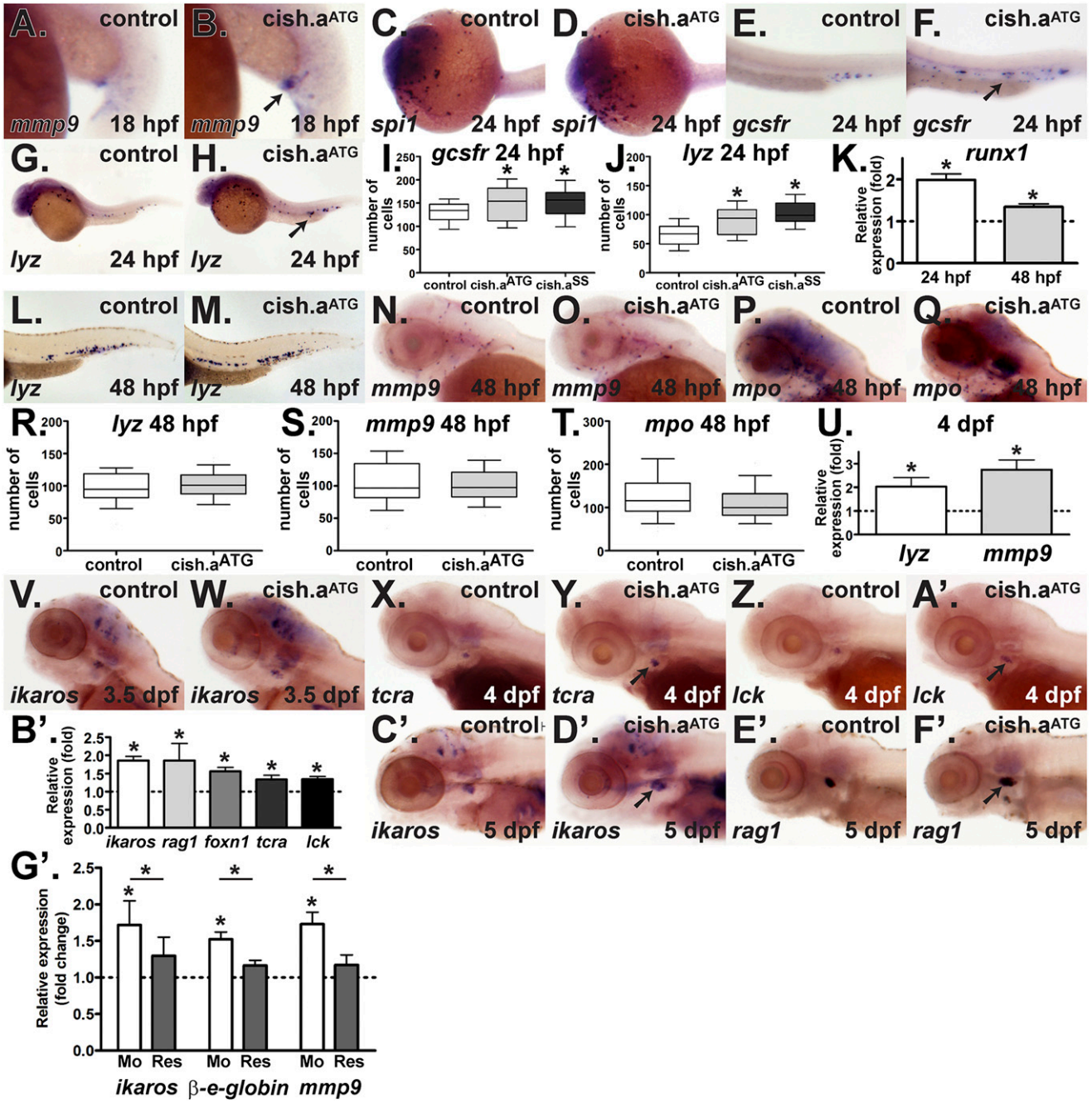

FIGURE 4. Effect of *cish.a* knockdown on myeloid and lymphoid markers. (**A**–**H**, **L**–**Q**, **V**–**Z**, **A′**, and **C′**–**F′**) WISH analysis of morphant embryos. Embryos injected with standard control (control) or cish.a morpholinos were subjected to WISH at the time points and with the probes indicated. Embryos are of lateral view with anterior to the left. Arrows indicate increased staining in cish.a morphants, with embryos shown being representative of $n > 150$ in each case, derived from at least three independent experiments. (**I**, **J**, and **R**–**T**) Quantitation of WISH staining. The numbers of discrete positive cells were determined for at least 30 embryos from a representative experiment for standard control and *cish.a* morphant groups for the marker/time point combinations indicated. Data are presented as a box-and-whiskers graph showing mean and range with statistically significant differences indicated ($*p < 0.05$). (**K**, **U**, **B′**, and **G′**) qRT^2-PCR analysis of marker genes at the times indicated in cish.a morphants relative to controls (K, U, and B′), or additionally in embryos injected with cish.a morpholino (Mo) alone or coinjected with morpholino-resistant *cish.a* mRNA (Res) (G′).

the *cish.a* and *cish.b* designations are consistent with the Zebrafish Nomenclature Committee guidelines and should take precedence. Indeed, the identification of two zebrafish *CISH* paralogs is especially significant, given that both the *JAK2* and *STAT5* genes are also duplicated in zebrafish (37, 38, 40). Whether this reflects functional redundancy or specification into distinct pathways is an important question for further study.

SOCS genes are generally transcribed at low levels in unstimulated cells, but upon cytokine stimulation their transcription rapidly increases (5), which for mammalian *CISH* genes is known to be largely dependent on STAT5 (8). Analysis of the *cish.a* promoter revealed conservation of two sets of tandem STAT5 sites, including one that has been shown to mediate tetrameric binding of STAT5 in mammals (14). DNA binding assays confirmed that zebrafish stat5.1 could bind to these sites in vitro. Moreover, expression of a constitutively active version of stat5.1 was able to significantly induce *cish.a* expression in vivo, whereas stat5.1 knockdown or application of a JAK2 inhibitor reduced *cish.a* levels. As a corollary, *Stat5a/b-*

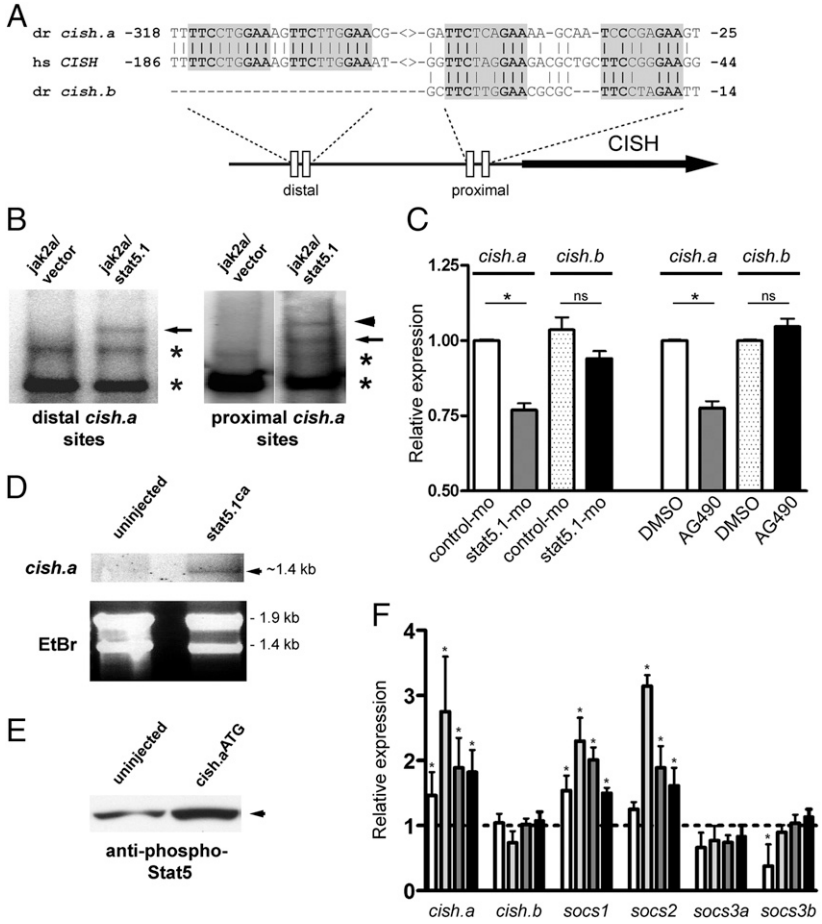

FIGURE 5. Interaction between cish.a and the JAK2/STAT5 pathway. (**A**) Conservation of STAT5 binding sites in *cish* promoters. Schematic representation of the human CISH gene and promoter with proximal and distal pairs of STAT5 binding sites boxed. The sequence around each pair is aligned with relevant *cish.a* and *cish.b* promoter sequences, with identical bases indicated and the consensus STAT5 binding sites ($TTCN_3GAA$) bolded and shaded. (**B**) Binding of stat5.1 to the *cish.a* promoter sites. Nuclear extracts from HEK293T cells cotransfected with an expression vector encoding hyperactive (E629K) jak2a and either empty vector or one expressing wild-type stat5.1 were analyzed by EMSA with proximal and distal STAT5 sites from the *cish.a* promoter. The arrows indicate the positions of the specific binding complexes, whereas asterisks indicate nonspecific complexes. (**C**) Regulation of *cish.a* expression by stat5.1 and jak2a. Total RNA was prepared from embryos injected with standard control or stat5.1 morpholino, and embryos were treated with vehicle (DMSO) or the JAK2 inhibitor AG490, and the expression of cish.a and cish.b was determined by qRT^2-PCR relative to expression of β-actin. (**D**) Induction of *cish.a* by stat5.1 in vivo. Total RNA was extracted at 24 hpf from uninjected wild-type embryos and embryos injected with RNA encoding constitutively active (ca) (H298R/N714F) zebrafish stat5.1, and separated on a formaldehyde agarose gel stained with ethidium bromide (EtBr) for visualization (*lower panel*) before Northern blot analysis using full-length zebrafish *cish.a* as a probe (*upper panel*). The arrowhead indicates the presence of the *cish.a* transcript in the injected sample at ~1400 bp, with the position of relevant size markers shown (*upper panel*). (**E**) Effect of *cish.a* knockdown on stat5 activation in vivo. Western blot of protein extracts from 30 pooled wild-type embryos (uninjected) or *cish.a* morphants ($cish.a^{ATG}$) using an anti–phospho-STAT5 Ab. (**F**) Effect of *cish.a* knockdown on the expression of *socs* genes. qRT^2-PCR analysis of standard control (control) or *cish.a* morphant embryos with primers specific for various *socs* family genes. In each case, expression was normalized relative to *β-actin*, with mean and SEM shown and statistical significance indicated ($*p < 0.05$).

defective mice showed no *Cish* expression (12, 13), suggesting that STAT5 activity is both necessary and sufficient to mediate expression of *Cish* in both species. Finally, increased STAT5 activity was observed in *cish.a* morphants, consistent with the reduced STAT5 activation observed in CISH-transgenic mice (8). Collectively, this suggests functional conservation of an in vivo JAK2/STAT5/CISH pathway across vertebrates.

Knockdown of *cish.a* produced a range of early hematopoietic phenotypes. Perturbation of the erythroid lineage was first observed as an increase in cells expressing zebrafish EPOR at 18 hpf, with a subsequent expansion throughout the erythroid cell lineage leading to increased hemoglobinized cells in circulation, which subsided from 48 hpf. The early myeloid lineage was also broadly expanded, including the population expressing the zebrafish G-CSFR, but again transiently. Finally, there was an increase in mature T cells. These phenotypes overlapped with those observed in zebrafish expressing constitutively active stat5.1 (46) or constitutively active jak2a (47), and they were also consistent with the effects on murine hematopoietic cells transduced with a constitutively active form of STAT5A (14). Interestingly, *Stat5a/b*-defective mice exhibited similar phenotypes to mice transgenic for CISH, including growth retardation, defective mammary gland development, and dysregulated T and NK cell development (12, 19, 20). These observations serve to emphasize the reciprocal regulation of STAT5 and CISH.

Erythropoiesis is controlled to a significant extent by the EPOR, which promotes erythroid progenitor cell proliferation and maturation, as well as preventing apoptosis of erythroid cells, a process that is tightly controlled via signaling through JAK2/STAT5 (2). It has previously been shown that CISH binds to Y401, and to a lesser extent Y344, on the EPOR and competes with STAT5 for these sites, thereby regulating the proliferation of erythroid cells (15). Additionally, enforced expression of CISH inhibited the

proliferation of EPO-dependent cell lines with a concomitant reduction in STAT5 activation (18, 19, 60) and increased apoptosis in fetal liver erythroid progenitor cells (18). However, the in vivo relevance of this biochemical interaction with EPOR has remained elusive, because neither group that generated transgenic mice overexpressing CISH reported erythroid defects (19, 20). Our study has shown definitively that ablation of *cish.a* resulted in the specific expansion of early erythroid cells, including the *epor*$^+$ compartment. Importantly, there is conservation of the CISH binding motif YxxL in zebrafish EPOR (39, 55) (Supplemental Fig. 2A). To our knowledge, this finding identifies CISH for the first time as a physiologic regulator of EPOR signaling and, along with other studies (47, 55), suggests that an epor/jak2a/stat5.1/cish.a pathway regulates embryonic erythropoiesis in zebrafish.

Embryonic myelopoiesis is controlled by a number of cytokine and growth factor receptors, with G-CSFR signaling playing an important and conserved role (3). Zebrafish gcsfr shows strong conservations with its mammalian counterparts (56), which are known to signal via JAK2/STAT5 (61) and be negatively regulated by CISH via two receptor tyrosines (10), both of which are conserved in the zebrafish gcsfr (Supplemental Fig. 2B). Moreover, ablation of *cish.a* led to expansion of the *gcsfr*$^+$ compartment, suggesting a negative regulatory role for *cish.a* in zebrafish gcsfr signaling in vivo, probably also via jak2a/stat5.1.

Multiple cytokine receptors participate in T cell development, principal among these being IL-2R, which strongly activates STAT5 (62). Transgenic mice expressing *CISH* from the β-actin promoter exhibited a reduction in the numbers of T NK cells and altered differentiation of Th1/Th2 cells by IL-2R, with activation of STAT5 by IL-2 being markedly reduced (19). Transgenic mice expressing *CISH* from the CD4 promoter also displayed moderately reduced T cell numbers despite prolonged T cell survival (20). The observed increase in mature T cells in *cish.a* morphants is consistent with a role for CISH in the physiologic regulation of IL-2R. This receptor complex is also conserved in zebrafish (39), including the region corresponding to residues 330–350 of the IL-2R β-chain where CISH has been shown to bind (63) (Supplemental Fig. 2C). Interestingly, zebrafish embryos expressing a constitutively active *stat5.1* also displayed a minor increase in T cells in the thymus (46).

In this study we have shown that reducing *cish.a* activity in zebrafish embryos results in perturbation of specific hematopoietic compartments in vivo, which, to our knowledge, provides the first clear insight into the normal developmental role of this gene. This work has also confirmed the tight reciprocal relationship between CISH and STAT5. Interestingly, the effects of *cish.a* knockdown were somewhat transient. This was not a consequence of using morpholinos, because the altered splicing of *cish.a* transcripts with cish.a^{SS} was sustained to 7 dpf (data not shown). However, enhanced expression of other zebrafish SOCS genes was observed in *cish.a* morphants, which might compensate for the loss of *cish.a*. This is particularly likely for the ortholog of SOCS1, which has been previously shown to regulate mammalian EPOR signaling (2), and the paralogs of SOCS3, which has been demonstrated to be a key in vivo regulator of G-CSFR (64). Indeed, we have previously demonstrated that zebrafish *socs1* functions during embryonic hematopoiesis (65). Other mechanisms that may contribute to this transient phenotype remain to be determined, and the role of the *cish.b* paralog awaits further study. Moreover, recent studies have also implicated the human *CISH* gene as a susceptibility locus for several infectious agents (22), and suggested that CISH contributes to expansion of regulatory T cells in response to microbial infection (66). Therefore, further analysis of the role of CISH in immunity represents an exciting area for future research.

Acknowledgments

We thank Daniel Merlo and Deakin University Upper Animal House staff for superb aquarium management, and Monique Trengove for critical reading of the manuscript and experimental expertise.

Disclosures

The authors have no financial conflicts of interest.

References

1. Robb, L. 2007. Cytokine receptors and hematopoietic differentiation. *Oncogene* 26: 6715–6723.
2. Richmond, T. D., M. Chohan, and D. L. Barber. 2005. Turning cells red: signal transduction mediated by erythropoietin. *Trends Cell Biol.* 15: 146–155.
3. Liongue, C., C. Wright, A. P. Russell, and A. C. Ward. 2009. Granulocyte colony-stimulating factor receptor: stimulating granulopoiesis and much more. *Int. J. Biochem. Cell Biol.* 41: 2372–2375.
4. Hilton, D. J., R. T. Richardson, W. S. Alexander, E. M. Viney, T. A. Willson, N. S. Sprigg, R. Starr, S. E. Nicholson, D. Metcalf, and N. A. Nicola. 1998. Twenty proteins containing a C-terminal SOCS box form five structural classes. *Proc. Natl. Acad. Sci. USA* 95: 114–119.
5. Wormald, S., and D. J. Hilton. 2004. Inhibitors of cytokine signal transduction. *J. Biol. Chem.* 279: 821–824.
6. O'Sullivan, L. A., C. Liongue, R. S. Lewis, S. E. M. Stephenson, and A. C. Ward. 2007. Cytokine receptor signaling through the Jak-Stat-Socs pathway in disease. *Mol. Immunol.* 44: 2497–2506.
7. Yoshimura, A., T. Ohkubo, T. Kiguchi, N. A. Jenkins, D. J. Gilbert, N. G. Copeland, T. Hara, and A. Miyajima. 1995. A novel cytokine-inducible gene CIS encodes an SH2-containing protein that binds to tyrosine-phosphorylated interleukin 3 and erythropoietin receptors. *EMBO J.* 14: 2816–2826.
8. Matsumoto, A., M. Masuhara, K. Mitsui, M. Yokouchi, M. Ohtsubo, H. Misawa, A. Miyajima, and A. Yoshimura. 1997. CIS, a cytokine inducible SH2 protein, is a target of the JAK-STAT5 pathway and modulates STAT5 activation. *Blood* 89: 3148–3154.
9. Adams, T. E., J. A. Hansen, R. Starr, N. A. Nicola, D. J. Hilton, and N. Billestrup. 1998. Growth hormone preferentially induces the rapid, transient expression of SOCS-3, a novel inhibitor of cytokine receptor signaling. *J. Biol. Chem.* 273: 1285–1287.
10. Hunter, M. G., A. Jacob, L. C. O'donnell, A. Agler, L. J. Druhan, K. M. Coggeshall, and B. R. Avalos. 2004. Loss of SHIP and CIS recruitment to the granulocyte colony-stimulating factor receptor contribute to hyperproliferative responses in severe congenital neutropenia/acute myelogenous leukemia. *J. Immunol.* 173: 5036–5045.
11. Helman, D., Y. Sandowski, Y. Cohen, A. Matsumoto, A. Yoshimura, S. Merchav, and A. Gertler. 1998. Cytokine-inducible SH2 protein (CIS3) and JAK2 binding protein (JAB) abolish prolactin receptor-mediated STAT5 signaling. *FEBS Lett.* 441: 287–291.
12. Teglund, S., C. McKay, E. Schuetz, J. M. van Deursen, D. Stravopodis, D. Wang, M. Brown, S. Bodner, G. Grosveld, and J. N. Ihle. 1998. Stat5a and Stat5b proteins have essential and nonessential, or redundant, roles in cytokine responses. *Cell* 93: 841–850.
13. Moriggl, R., V. Sexl, R. Piekorz, D. Topham, and J. N. Ihle. 1999. Stat5 activation is uniquely associated with cytokine signaling in peripheral T cells. *Immunity* 11: 225–230.
14. Moriggl, R., V. Sexl, L. Kenner, C. Duntsch, K. Stangl, S. Gingras, A. Hoffmeyer, A. Bauer, R. Piekorz, D. Wang, et al. 2005. Stat5 tetramer formation is associated with leukemogenesis. *Cancer Cell* 7: 87–99.
15. Verdier, F., S. Chretien, O. Muller, P. Varlet, A. Yoshimura, S. Gisselbrecht, C. Lacombe, and P. Mayeux. 1998. Proteasomes regulate erythropoietin receptor and signal transducer and activator of transcription 5 (STAT5) activation. Possible involvement of the ubiquitinated Cis protein. *J. Biol. Chem.* 273: 28185–28190.
16. Ram, P. A., and D. J. Waxman. 1999. SOCS/CIS protein inhibition of growth hormone-stimulated STAT5 signaling by multiple mechanisms. *J. Biol. Chem.* 274: 35553–35561.
17. Piessevaux, J., L. De Ceuninck, D. Catteeuw, F. Peelman, and J. Tavernier. 2008. Elongin B/C recruitment regulates substrate binding by CIS. *J. Biol. Chem.* 283: 21334–21346.
18. Ketteler, R., C. S. Moghraby, J. G. Hsiao, O. Sandra, H. F. Lodish, and U. Klingmüller. 2003. The cytokine-inducible Scr homology domain-containing protein negatively regulates signaling by promoting apoptosis in erythroid progenitor cells. *J. Biol. Chem.* 278: 2654–2660.
19. Matsumoto, A., Y. Seki, M. Kubo, S. Ohtsuka, A. Suzuki, I. Hayashi, K. Tsuji, T. Nakahata, M. Okabe, S. Yamada, and A. Yoshimura. 1999. Suppression of STAT5 functions in liver, mammary glands, and T cells in cytokine-inducible SH2-containing protein 1 transgenic mice. *Mol. Cell. Biol.* 19: 6396–6407.
20. Li, S., S. Chen, X. Xu, A. Sundstedt, K. M. Paulsson, P. Anderson, S. Karlsson, H. O. Sjögren, and P. Wang. 2000. Cytokine-induced Src homology 2 protein (CIS) promotes T cell receptor-mediated proliferation and prolongs survival of activated T cells. *J. Exp. Med.* 191: 985–994.
21. Endo, T., A. Sasaki, M. Minoguchi, A. Joo, and A. Yoshimura. 2003. CIS1 interacts with the Y532 of the prolactin receptor and suppresses prolactin-dependent STAT5 activation. *J. Biochem.* 133: 109–113.

22. Khor, C. C., F. O. Vannberg, S. J. Chapman, H. Guo, S. H. Wong, A. J. Walley, D. Vukcevic, A. Rautanen, T. C. Mills, K. C. Chang, et al. 2010. CISH and susceptibility to infectious diseases. *N. Engl. J. Med.* 362: 2092–2101.
23. Yang, X. O., H. Zhang, B. S. Kim, X. Niu, J. Peng, Y. Chen, R. Kerketta, Y. H. Lee, S. H. Chang, D. B. Corry, et al. 2013. The signaling suppressor CIS controls proallergic T cell development and allergic airway inflammation. *Nat. Immunol.* 14: 732–740.
24. Martin, C. S., A. Moriyama, and L. I. Zon. 2011. Hematopoietic stem cells, hematopoiesis and disease: lessons from the zebrafish model. *Genome Med.* 3: 83.
25. Davidson, A. J., and L. I. Zon. 2004. The "definitive" (and "primitive") guide to zebrafish hematopoiesis. *Oncogene* 23: 7233–7246.
26. Patterson, L. J., M. Gering, C. E. Eckfeldt, A. R. Green, C. M. Verfaillie, S. C. Ekker, and R. Patient. 2007. The transcription factors Scl and Lmo2 act together during development of the hemangioblast in zebrafish. *Blood* 109: 2389–2398.
27. Willett, C. E., H. Kawasaki, C. T. Amemiya, S. Lin, and L. A. Steiner. 2001. Ikaros expression as a marker for lymphoid progenitors during zebrafish development. *Dev. Dyn.* 222: 694–698.
28. Lieschke, G. J., A. C. Oates, B. H. Paw, M. A. Thompson, N. E. Hall, A. C. Ward, R. K. Ho, L. I. Zon, and J. E. Layton. 2002. Zebrafish SPI-1 (PU.1) marks a site of myeloid development independent of primitive erythropoiesis: implications for axial patterning. *Dev. Biol.* 246: 274–295.
29. Long, Q., A. Meng, H. Wang, J. R. Jessen, M. J. Farrell, and S. Lin. 1997. *GATA-1* expression pattern can be recapitulated in living transgenic zebrafish using GFP reporter gene. *Development* 124: 4105–4111.
30. Liu, F., and Z. Wen. 2002. Cloning and expression pattern of the lysozyme C gene in zebrafish. *Mech. Dev.* 113: 69–72.
31. Brownlie, A., C. Hersey, A. C. Oates, B. H. Paw, A. M. Falick, H. E. Witkowska, J. Flint, D. Higgs, J. Jessen, N. Bahary, et al. 2003. Characterization of embryonic globin genes of the zebrafish. *Dev. Biol.* 255: 48–61.
32. Lieschke, G. J., A. C. Oates, M. O. Crowhurst, A. C. Ward, and J. E. Layton. 2001. Morphologic and functional characterization of granulocytes and macrophages in embryonic and adult zebrafish. *Blood* 98: 3087–3096.
33. Yoong, S., B. O'Connell, A. Soanes, M. O. Crowhurst, G. J. Lieschke, and A. C. Ward. 2007. Characterization of the zebrafish matrix metalloproteinase 9 gene and its developmental expression pattern. *Gene Expr. Patterns* 7: 39–46.
34. Murayama, E., K. Kissa, A. Zapata, E. Mordelet, V. Briolat, H.-F. Lin, R. I. Handin, and P. Herbomel. 2006. Tracing hematopoietic precursor migration to successive hematopoietic organs during zebrafish development. *Immunity* 25: 963–975.
35. Bertrand, J. Y., A. D. Kim, E. P. Violette, D. L. Stachura, J. L. Cisson, and D. Traver. 2007. Definitive hematopoiesis initiates through a committed erythromyeloid progenitor in the zebrafish embryo. *Development* 134: 4147–4156.
36. Danilova, N., V. S. Hohman, F. Sacher, T. Ota, C. E. Willett, and L. A. Steiner. 2004. T cells and the thymus in developing zebrafish. *Dev. Comp. Immunol.* 28: 755–767.
37. Oates, A. C., A. Brownlie, S. J. Pratt, D. V. Irvine, E. C. Liao, B. H. Paw, K. J. Dorian, S. L. Johnson, J. H. Postlethwait, L. I. Zon, and A. F. Wilks. 1999. Gene duplication of zebrafish JAK2 homologs is accompanied by divergent embryonic expression patterns: only jak2a is expressed during erythropoiesis. *Blood* 94: 2622–2636.
38. Lewis, R. S., and A. C. Ward. 2004. Conservation, duplication and divergence of the zebrafish stat5 genes. *Gene* 338: 65–74.
39. Liongue, C., and A. C. Ward. 2007. Evolution of class I cytokine receptors. *BMC Evol. Biol.* 7: 120.
40. Liongue, C., L. A. O'Sullivan, M. C. Trengove, and A. C. Ward. 2012. Evolution of JAK-STAT pathway components: mechanisms and role in immune system development. *PLoS ONE* 7: e32777.
41. Altschul, S. F., T. L. Madden, A. A. Schäffer, J. Zhang, Z. Zhang, W. Miller, and D. J. Lipman. 1997. Gapped BLAST and PSI-BLAST: a new generation of protein database search programs. *Nucleic Acids Res.* 25: 3389–3402.
42. Jeanmougin, F., J. D. Thompson, M. Gouy, D. G. Higgins, and T. J. Gibson. 1998. Multiple sequence alignment with Clustal X. *Trends Biochem. Sci.* 23: 403–405.
43. Perrière, G., and M. Gouy. 1996. WWW-query: an on-line retrieval system for biological sequence banks. *Biochimie* 78: 364–369.
44. Page, R. D. 1996. TreeView: an application to display phylogenetic trees on personal computers. *Comput. Appl. Biosci.* 12: 357–358.
45. Padgett, R. A., P. J. Grabowski, M. M. Konarska, S. Seiler, and P. A. Sharp. 1986. Splicing of messenger RNA precursors. *Annu. Rev. Biochem.* 55: 1119–1150.
46. Lewis, R. S., S. E. M. Stephenson, and A. C. Ward. 2006. Constitutive activation of zebrafish Stat5 expands hematopoietic cell populations in vivo. *Exp. Hematol.* 34: 179–187.
47. Ma, A. C., A. C. Ward, R. Liang, and A. Y. Leung. 2007. The role of jak2a in zebrafish hematopoiesis. *Blood* 110: 1824–1830.
48. Onnebo, S. M. N., M. M. Condron, D. O. McPhee, G. J. Lieschke, and A. C. Ward. 2005. Hematopoietic perturbation in zebrafish expressing a *tel-jak2a* fusion. *Exp. Hematol.* 33: 182–188.
49. Abramoff, M., P. Magelhaes, and S. Ram. 2004. Image processing with ImageJ. *Biophotonics Int.* 11: 36–42.
50. Zhu, H., D. Traver, A. J. Davidson, A. Dibiase, C. Thisse, B. Thisse, S. Nimer, and L. I. Zon. 2005. Regulation of the lmo2 promoter during hematopoietic and vascular development in zebrafish. *Dev. Biol.* 281: 256–269.
51. Liao, E. C., B. H. Paw, A. C. Oates, S. J. Pratt, J. H. Postlethwait, and L. I. Zon. 1998. SCL/Tal-1 transcription factor acts downstream of cloche to specify hematopoietic and vascular progenitors in zebrafish. *Genes Dev.* 12: 621–626.
52. Kalev-Zylinska, M. L., J. A. Horsfield, M. V. Flores, J. H. Postlethwait, M. R. Vitas, A. M. Baas, P. S. Crosier, and K. E. Crosier. 2002. Runx1 is required for zebrafish blood and vessel development and expression of a human RUNX1-CBF2T1 transgene advances a model for studies of leukemogenesis. *Development* 129: 2015–2030.
53. Kobayashi, M., K. Nishikawa, and M. Yamamoto. 2001. Hematopoietic regulatory domain of gata1 gene is positively regulated by GATA1 protein in zebrafish embryos. *Development* 128: 2341–2350.
54. Ward, A. C., D. O. McPhee, M. M. Condron, S. Varma, S. H. Cody, S. M. N. Onnebo, B. H. Paw, L. I. Zon, and G. J. Lieschke. 2003. The zebrafish *spi1* promoter drives myeloid-specific expression in stable transgenic fish. *Blood* 102: 3238–3240.
55. Paffett-Lugassy, N., N. Hsia, P. G. Fraenkel, B. Paw, I. Leshinsky, B. Barut, N. Bahary, J. Caro, R. Handin, and L. I. Zon. 2007. Functional conservation of erythropoietin signaling in zebrafish. *Blood* 110: 2718–2726.
56. Liongue, C., C. J. Hall, B. A. O'Connell, P. Crosier, and A. C. Ward. 2009. Zebrafish granulocyte colony-stimulating factor receptor signaling promotes myelopoiesis and myeloid cell migration. *Blood* 113: 2535–2546.
57. Willett, C. E., A. G. Zapata, N. Hopkins, and L. A. Steiner. 1997. Expression of zebrafish rag genes during early development identifies the thymus. *Dev. Biol.* 182: 331–341.
58. Danilova, N., A. Visel, C. E. Willett, and L. A. Steiner. 2004. Expression of the winged helix/forkhead gene, *foxn4*, during zebrafish development. *Brain Res. Dev. Brain Res.* 153: 115–119.
59. Jin, H. J., J. Z. Shao, L. X. Xiang, H. Wang, and L. L. Sun. 2008. Global identification and comparative analysis of SOCS genes in fish: insights into the molecular evolution of SOCS family. *Mol. Immunol.* 45: 1258–1268.
60. Jegalian, A. G., and H. Wu. 2002. Differential roles of SOCS family members in EpoR signal transduction. *J. Interferon Cytokine Res.* 22: 853–860.
61. Ward, A. C. 2007. The role of the granulocyte colony-stimulating factor receptor (G-CSF-R) in disease. *Front. Biosci.* 12: 608–618.
62. Burchill, M. A., J. Yang, K. B. Vang, and M. A. Farrar. 2007. Interleukin-2 receptor signaling in regulatory T cell development and homeostasis. *Immunol. Lett.* 114: 1–8.
63. Aman, M. J., T. S. Migone, A. Sasaki, D. P. Ascherman, Mh. Zhu, E. Soldaini, K. Imada, A. Miyajima, A. Yoshimura, and W. J. Leonard. 1999. CIS associates with the interleukin-2 receptor β chain and inhibits interleukin-2-dependent signaling. *J. Biol. Chem.* 274: 30266–30272.
64. Hörtner, M., U. Nielsch, L. M. Mayr, J. A. Johnston, P. C. Heinrich, and S. Haan. 2002. Suppressor of cytokine signaling-3 is recruited to the activated granulocyte-colony stimulating factor receptor and modulates its signal transduction. *J. Immunol.* 169: 1219–1227.
65. O'Sullivan, L. A., S. M. Noor, M. C. Trengove, R. S. Lewis, C. Liongue, N. S. Sprigg, S. E. Nicholson, and A. C. Ward. 2011. Suppressor of cytokine signaling 1 regulates embryonic myelopoiesis independently of its effects on T cell development. *J. Immunol.* 186: 4751–4761.
66. Periasamy, S., R. Dhiman, P. F. Barnes, P. Paidipally, A. Tvinnereim, A. Bandaru, V. L. Valluri, and R. Vankayalapati. 2011. Programmed death 1 and cytokine inducible SH2-containing protein dependent expansion of regulatory T cells upon stimulation With *Mycobacterium tuberculosis*. *J. Infect. Dis.* 203: 1256–1263.